High-Mass SUSY Models at LHC and VLHC: Part II

I. Hinchliffe*
Lawrence Berkeley National Laboratory, Berkeley, CA
F.E. Paige†
Brookhaven National Laboratory, Upton, NY

Signatures at the LHC and VLHC are examined for SUSY models consistent with existing constraints and having very heavy masses.

This note continues the discussion of the SUSY models of Ref [1]. The reader should consult [2] for the introductory material. This note is concerned with Point H (see Table 1 of[2]) and some brief remarks regarding the lower mass points. Point H is able to accommodate very sparticles and be consistent without overclosing the universe as the destruction rate for the $\tilde{\chi}_1^0$ is enhanced by coannihilation region with a stau. This implies a very small splitting between the $\tilde{\tau}_1$ and the $\tilde{\chi}_1^0$. In this particular case, $\tilde{\tau}_1 \not\to \tilde{\chi}_1^0\tau$, so it must decay by second order weak processes, $\tilde{\tau}_1 \to \tilde{\chi}_1^0 e\bar{\nu}_e\nu_\tau$, giving a long lifetime. The dominant SUSY rates are the strong production of valance squarks, with $\tilde{q}_L \to \tilde{\chi}_1^\pm q, \tilde{\chi}_2^0 q$ and $\tilde{q}_R \to \tilde{\chi}_1^0$. The stau which are produced from cascade decays of these squarks, then exit the detector with a signal similar to a "heavy muon."

The p_T spectrum of these quasi-stable $\tilde{\tau}_1$ for $1000\,\mathrm{fb}^{-1}$ is shown in Figure 1. The ATLAS muon system [3] has a time resolution of about 0.7 ns for time of flight over a cylinder of radius 10 m and half-length 20 m. The spectrum with a time delay $\Delta t > 10\sigma\,(7\,\mathrm{ns})$ is also shown. Notice that this signal could be observed at the LHC with $\sim 300\,\mathrm{fb}^{-1}$. Triggering on a slow $\tilde{\tau}_1$ may be a problem since the time-window for the trigger chambers is limited. However, the $\not{E}_T$ in SUSY events as measured by the calorimeter is quite large as shown in Figure 2. It probably is possible to trigger just on jets plus $\not{E}_T$, the distribution for which is shown in Figure 2. The mass of the stable stau can be measured by exploiting the time of flight measurements in the muon measurement

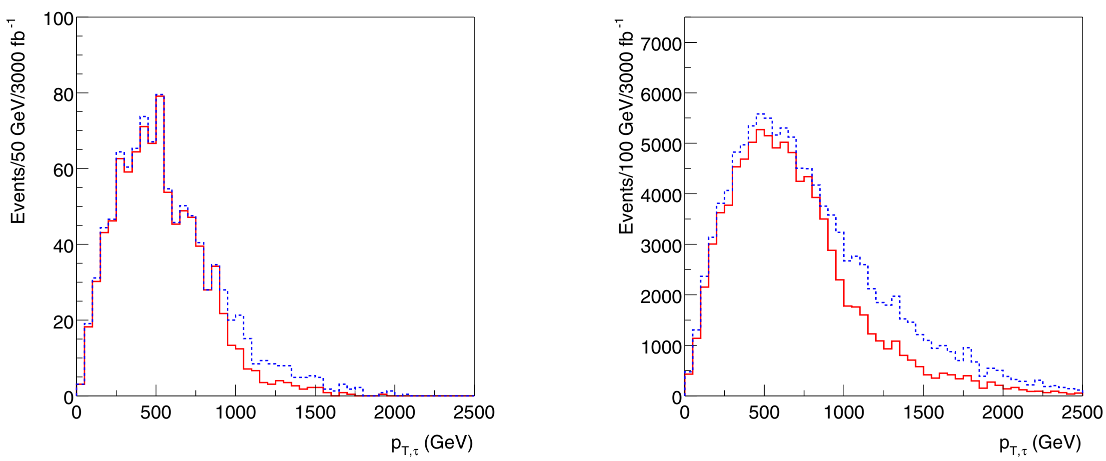

Figure 1: p_T distribution of $\tilde{\tau}_1$ at SLHC (left) and VLHC (right) for Point H. Dashed: all $\tilde{\tau}_1$. Solid: $\tilde{\tau}_1$ with $\Delta t > 7\,\mathrm{ns}$

---

*I_Hinchliffe@lbl.gov; The work was supported in part by the Director, Office of Energy Research, Office of High Energy and Nuclear Physics of the U.S. Department of Energy under Contract DE-AC03-76SF00098.
†paige@bnl.gov; The work was supported in part by the Director, Office of Energy Research, Office of High Energy and Nuclear Physics of the U.S. Department of Energy under Contract DE-AC02-98CH10886.

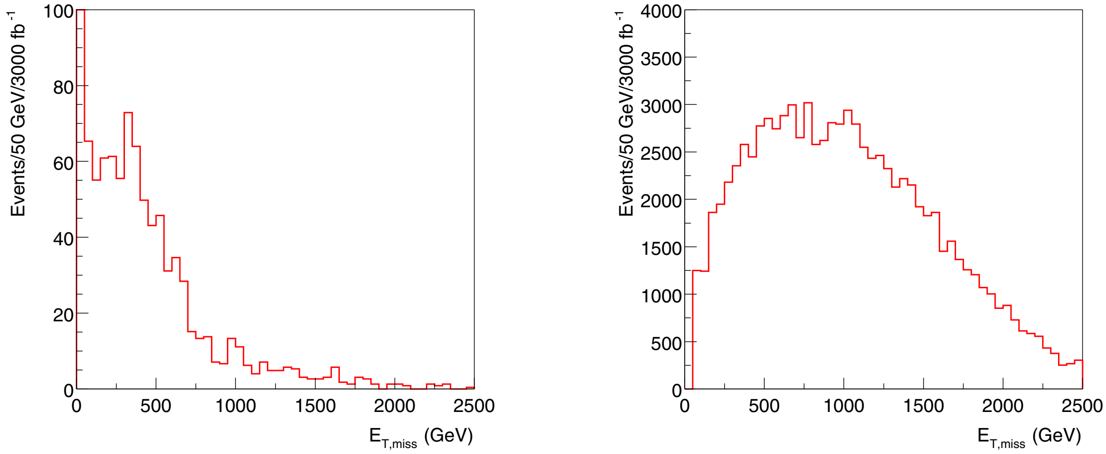

Figure 2: Calorimetric $\not{E}_T$ distributions in $\tilde{\tau}_1$ events for SLHC (left) and VLHC (right) for Point H.

system. Studies of such quasi stable particles at somewhat smaller masses carried out or the ATLAS detector showed a mass resolution of approximately 3% given sufficient statistics (see Section 20.3.4.2 of [3]). A precision of this order should be achievable with 3000 fb^{-1} at either the LHC or VLHC. One can then build on the stable stau to reconstruct the decay chain using techniques similar to those used for the GMSB studies [3, 4]. This is not pursued here.

The stable τ_1 signature is somewhat exceptional so we explore other signatures that do not require it and would be present if the stau decayed inside the detector. For such high masses the strong production is mainly of $\tilde{u}$ and $\tilde{d}$. Events are selected with hadronic jets and missing E_T and the following scalar quantity formed

$$M_{\rm eff} = \not{E}_T + \sum_{\rm jets} E_{T,{\rm jet}} + \sum_{\rm leptons} E_{T,{\rm lepton}}$$

where the sum runs over all jets with $E_T > 50$ GeV and $|\eta| < 5.0$ and isolated leptons with $E_T > 15$ GeV and$|\eta| < 2.5$. To optimize this signature, events were further selected with at least two jets with $p_T > 0.1M_{\rm eff}$, $\not{E}_T > 0.3M_{\rm eff}$, $\Delta\phi(j_0, \not{E}_T) < \pi - 0.2$, and $\Delta\phi(j_0, j_1) < 2\pi/3$. The $M_{\rm eff}$ distributions with these cuts for the SLHC and the VLHC are shown in Figure 3. Note that at the SLHC the number of events in the region where $S/B > 1$ is small. Given the uncertainties in the modeling of the standard model backgrounds the shower Monte Carlo, it is not possible to claim that the SLHC could see a signal. The VLHC should have no difficulty.

Dileptons arise from the cascade $\tilde{q}_L \to q\tilde{\chi}_2^0 \to q\ell^+\ell^-\tilde{\chi}_1^0$, The dilepton mass distributions should have a kinematic endpoint corresponding to this decay. Figure 4 shows the distribution for same flavor and different flavor lepton pairs. Events were required to have $M_{\rm eff} > 3000$ GeV and $\not{E}_T > 0.2M_{\rm eff}$ and to have two isolated opposite sign leptons with $E_T > 15$ GeV and $|\eta| < 2.5$. The structure at the VLHC is clear; the edge comes mainly from $\tilde{\chi}_2^0 \to \tilde{\ell}_L^{\pm}\ell^{\mp}$, which has a branching ratio of 15% per flavor. This gives an endpoint at

$$\sqrt{\frac{(M^2_{\tilde{\chi}_2^0} - M^2_{\tilde{\ell}_L})(M^2_{\tilde{\ell}_L} - M^2_{\tilde{\chi}_1^0})}{M^2_{\tilde{\ell}_L}}} = 447.3\,\text{GeV}$$

consistent with the observed endpoint in Figure 4. Of course this plot does not distinguish $\tilde{\ell}_L$ and $\tilde{\ell}_R$. In the case of the upgraded LHC, the signal may be observable, but it should be noted that the background is uncertain as only three generated events passed the cuts.

If the stable stau is used then the situation improves considerably. The dilepton mass for events containing a $\tilde{\tau}_1$ with a time delay $7 < \Delta t < 21.5$ ns is shown in Figure 5. Since $\Delta t > 10\sigma$, the standard model background is expected to be negligible. The SLHC signal is improved and a measurement may now be possible. The acceptance for VLHC is somewhat worse than the inclusive sample, but having the correlation of the dileptons with the $\tilde{\tau}_1$ should be useful.

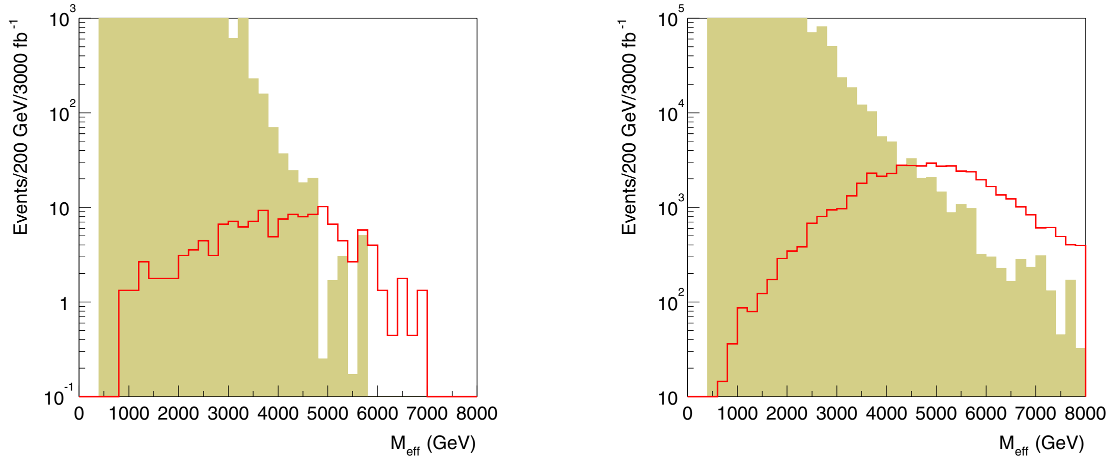

Figure 3: M_{eff} distribution for SLHC (left) and VLHC (right) for Point H. Solid: signal. Shaded: SM background.

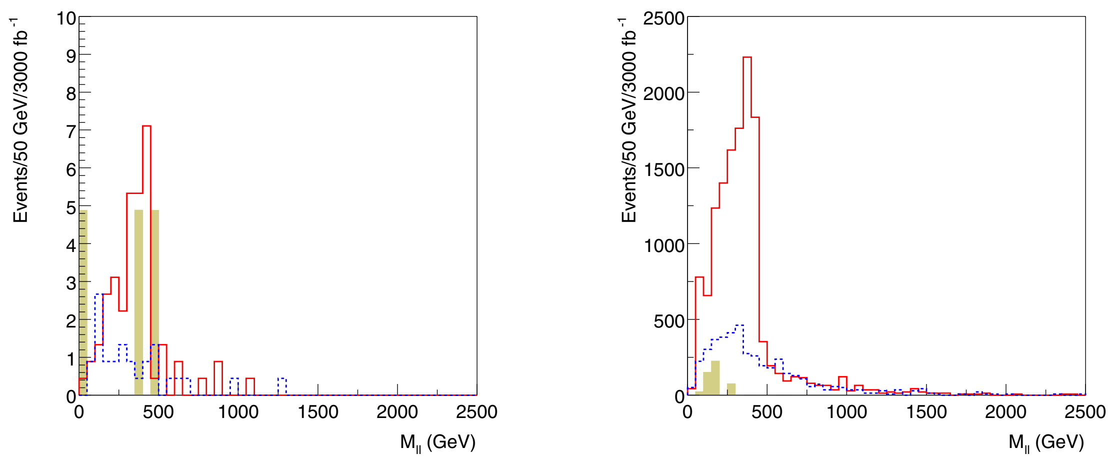

Figure 4: $M_{\ell\ell}$ distribution for SLHC (left) and VLHC (right) for Point H. Solid: $\ell^+\ell^-$. Dashed: $e^\pm\mu^\mp$.

The VLHC gives a gain of ~ 100 in statistics over the LHC for the same luminosity at this point, which is at the limit of observability at the LHC. If the VLHC luminosity were substantially lower, the improvement provided by it would be rather marginal. The cross section increases by another factor of ~ 100 at 200 TeV.

The Points A, B, C, D, G, I, and L are similar to the "Point 5" or "Point 6" analysis of [3] in that lepton structure from the decay $\tilde{\chi}_2^0 \to \tilde{\ell}_R\ell \to \ell^+\ell^-\tilde{\chi}_1^0$ and/or $\tilde{\chi}_2^0 \to t\tilde{a}u\tau \to \tau^+\tau^-\tilde{\chi}_1^0$ is present. In most cases decay $\tilde{\chi}_2^0 \to \tilde{\ell}_L\ell$ is also allowed, so that a more complicated dilepton mass spectrum is observable. This should enable the extraction of m_{ℓ_L} in addition (for an example see Figure 20–53 of [3]). Points A, D and L have higher squark/gluino masses and will require more integrated luminosity. Nevertheless one can have confidence that the baseline LHC will make many measurements in all of these cases.

The work was supported in part by the Director, Office of Energy Research, Office of High Energy and Nuclear Physics of the U.S. Department of Energy under Contracts DE–AC03–76SF00098 and DE-AC02-98CH10886. Accordingly, the U.S. Government retains a nonexclusive, royalty-free license to publish or reproduce the published form of this contribution, or allow others to do so, for U.S. Government purposes.

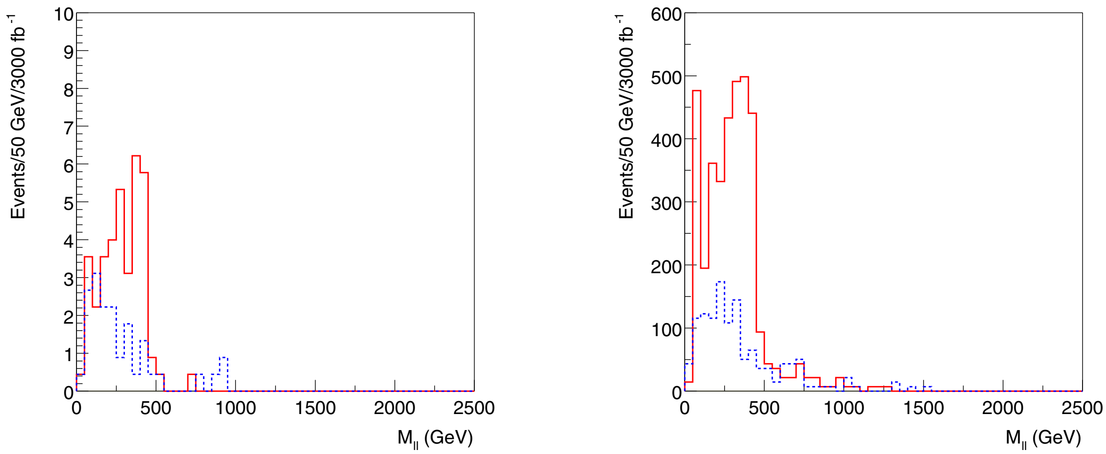

Figure 5: $M_{\ell\ell}$ distribution for SLHC (left) and VLHC (right) for events containing a $\tilde{\tau}_1$ for Point H. Solid: $\ell^+\ell^-$. Dashed: $e^\pm\mu^\mp$.

References

[1] M. Battaglia *et al.*, hep-ph/0106204.
[2] I. Hinchliffe and F. E. Paige (in preparation)
[3] ATLAS Collaboration, *ATLAS Detector and Physics Performance Technical Design Report*, CERN/LHCC/99-14, `http://atlasinfo.cern.ch/Atlas/GROUPS/PHYSICS/TDR/-access.html`.
[4] I. Hinchliffe and F. E. Paige, Phys. Rev. D **60**, 095002 (1999)